

SEARCH FOR NEW BARYON RESONANCES

Bijan Saghai

*Service de Physique Nucléaire, DAPNIA - CEA/Saclay,
F-91191 Gif-sur-Yvette Cedex, France
E-mail: bsaghai@cea.fr*

Zhenping Li

Physics Department, Peking University, Beijing 100871, P.R. China

Within a chiral constituent quark formalism, allowing the inclusion of all known resonances, a comprehensive study of the recent η photoproduction data on the proton up to $E_\gamma^{lab} \approx 2$ GeV is performed. This study shows evidence for a new S_{11} resonances and indicates the presence of an additional missing P_{13} resonance.

1 Introduction

For several decades, the baryon resonances have been investigated¹ mainly through partial wave analysis of the “pionic” processes $\pi N \rightarrow \pi N$, ηN , $\gamma N \rightarrow \pi N$, and to less extent, from two pion final states.

Recent advent of high quality electromagnetic beams and sophisticated detectors, has boosted intensive experimental and theoretical study of mesons photo- and electro-production. One of the exciting topics is the search for new baryon resonances which do not couple or couple too weakly to the πN channel. Several such resonances have been predicted^{2,3,4} by different QCD-inspired approaches, offering strong test of the underlying concepts.

Investigation of η -meson production *via* electromagnetic probes offers access to fundamental information in hadrons spectroscopy. The properties of the decay of baryon resonances into γN and/or $N^* \rightarrow \eta N$ are intimately related to their internal structure^{3,5,6}. Extensive recent experimental efforts on η photoproduction^{7,8,9,10,11} are opening a new era in this topic.

The focus in this manuscript is to study all the recent $\gamma p \rightarrow \eta p$ data for $E_\gamma^{lab} < 2$ GeV ($W \equiv E_{total}^{cm} < 2.2$ GeV) within a chiral constituent quark formalism based on the $SU(6) \otimes O(3)$ symmetry. The advantage of the quark model for meson photoproduction is the ability to relate the photoproduction data directly to the internal structure of the baryon resonances. Moreover, this approach allows the inclusion of all of the known baryon resonances. To go beyond the exact $SU(6) \otimes O(3)$ symmetry, we introduce^{12,13} symmetry breaking factors and relate them to the configuration mixing angles generated by the gluon exchange interactions in the quark model⁵.

2 Theoretical Frame

The chiral constituent quark approach for meson photoproduction is based on the low energy QCD Lagrangian¹⁴

$$\mathcal{L} = \bar{\psi} [\gamma_\mu (i\partial^\mu + V^\mu + \gamma_5 A^\mu) - m] \psi + \dots \quad (1)$$

where ψ is the quark field in the $SU(3)$ symmetry, $V^\mu = (\xi^\dagger \partial_\mu \xi + \xi \partial_\mu \xi^\dagger)/2$ and $A^\mu = i(\xi^\dagger \partial_\mu \xi - \xi \partial_\mu \xi^\dagger)/2$ are the vector and axial currents, respectively, with $\xi = e^{i\Pi f}$; f is a decay constant and Π the Goldstone boson field.

The four components for the photoproduction of pseudoscalar mesons based on the QCD Lagrangian are:

$$\mathcal{M}_{fi} = \mathcal{M}_{seagull} + \mathcal{M}_s + \mathcal{M}_u + \mathcal{M}_t \quad (2)$$

The first term in Eq. (2) is a seagull term. It is generated by the gauge transformation of the axial vector A_μ in the QCD Lagrangian. This term, being proportional to the electric charge of the outgoing mesons, does not contribute to the production of the η -meson. The second and the third terms correspond to the s - and u -channels, respectively. The last term is the t -channel contribution and contains two parts: *i*) charged meson exchanges which are proportional to the charge of outgoing mesons and thus do not contribute to the process $\gamma N \rightarrow \eta N$; *ii*) ρ and ω exchange in the η production which are excluded here due to the duality hypothesis¹³.

The u -channel contributions are divided into the nucleon Born term and the contributions from the excited resonances. The matrix elements for the nucleon Born term are given explicitly, while the contributions from the excited resonances above 2 GeV for a given parity are assumed to be degenerate so that their contributions could be written in a compact form¹⁵.

The contributions from the s -channel resonances can be written as

$$\mathcal{M}_{N^*} = \frac{2M_{N^*}}{s - M_{N^*} [M_{N^*} - i\Gamma(q)]} e^{-\frac{k^2+q^2}{6\alpha_{ho}^2}} \mathcal{A}_{N^*}, \quad (3)$$

where $k = |\mathbf{k}|$ and $q = |\mathbf{q}|$ represent the momenta of the incoming photon and the outgoing meson respectively, \sqrt{s} is the total energy of the system, $e^{-(k^2+q^2)/6\alpha_{ho}^2}$ is a form factor in the harmonic oscillator basis with the parameter α_{ho}^2 related to the harmonic oscillator strength in the wave-function, and M_{N^*} and $\Gamma(q)$ are the mass and the total width of the resonance, respectively. The amplitudes \mathcal{A}_{N^*} are divided into two parts^{15,16}: the contribution from each resonance below 2 GeV, the transition amplitudes of which have been translated into the standard CGLN amplitudes in the harmonic oscillator basis,

Table 1: Resonances included in our study with their $SU(6) \otimes O(3)$ configuration assignments.

Resonance	$SU(6) \otimes O(3)$ State	C_{N^*}	Resonance	$SU(6) \otimes O(3)$ State	C_{N^*}
$S_{11}(1535)$	$N(^2P_M)_{\frac{1}{2}-}$	1	$S_{11}(1650)$	$N(^4P_M)_{\frac{1}{2}-}$	0
$P_{11}(1440)$	$N(^2S'_S)_{\frac{1}{2}+}$	1	$P_{11}(1710)$	$N(^2S_M)_{\frac{1}{2}+}$	1
$P_{13}(1720)$	$N(^2D_S)_{\frac{3}{2}+}$	1	$P_{13}(1900)$	$N(^2D_M)_{\frac{3}{2}+}$	1
$D_{13}(1520)$	$N(^2P_M)_{\frac{3}{2}-}$	1	$D_{13}(1700)$	$N(^4P_M)_{\frac{3}{2}-}$	0
$F_{15}(1680)$	$N(^2D_S)_{\frac{5}{2}+}$	1	$F_{15}(2000)$	$N(^2D_M)_{\frac{5}{2}+}$	1
			$D_{15}(1675)$	$N(^4P_M)_{\frac{5}{2}-}$	0

and the contributions from the resonances above 2 GeV treated as degenerate, since little experimental information is available on those resonances.

The contributions from each resonance to η photoproduction is determined by introducing¹² a new set of parameters C_{N^*} and the following substitution rule for the amplitudes \mathcal{A}_{N^*} ,

$$\mathcal{A}_{N^*} \rightarrow C_{N^*} \mathcal{A}_{N^*}, \quad (4)$$

so that

$$\mathcal{M}_{N^*}^{exp} = C_{N^*}^2 \mathcal{M}_{N^*}^{qm}, \quad (5)$$

where $\mathcal{M}_{N^*}^{exp}$ is the experimental value of the observable, and $\mathcal{M}_{N^*}^{qm}$ is calculated in the quark model¹⁶. The $SU(6) \otimes O(3)$ symmetry predicts $C_{N^*} = 0$ for $S_{11}(1650)$, $D_{13}(1700)$, and $D_{15}(1675)$ resonances, and $C_{N^*} = 1$ for other resonances in Table 1. Thus, the coefficients C_{N^*} give a measure of the discrepancies between the theoretical results and the experimental data and show the extent to which the $SU(6) \otimes O(3)$ symmetry is broken in the process investigated here.

One of the main reasons that the $SU(6) \otimes O(3)$ symmetry is broken is due to the configuration mixings caused by the one gluon exchange⁵. Here, the most relevant configuration mixings are those of the two S_{11} and the two D_{13} states around 1.5 to 1.7 GeV. The configuration mixings can be expressed in terms of the mixing angle between the two $SU(6) \otimes O(3)$ states $|N(^2P_M) \rangle$ and $|N(^4P_M) \rangle$, with the total quark spin 1/2 and 3/2,

$$\begin{pmatrix} |S_{11}(1535) \rangle \\ |S_{11}(1650) \rangle \end{pmatrix} = \begin{pmatrix} \cos \theta_S & -\sin \theta_S \\ \sin \theta_S & \cos \theta_S \end{pmatrix} \begin{pmatrix} |N(^2P_M)_{\frac{1}{2}-} \rangle \\ |N(^4P_M)_{\frac{1}{2}-} \rangle \end{pmatrix}, \quad (6)$$

and

$$\begin{pmatrix} |D_{13}(1520)\rangle \\ |D_{13}(1700)\rangle \end{pmatrix} = \begin{pmatrix} \cos\theta_D & -\sin\theta_D \\ \sin\theta_D & \cos\theta_D \end{pmatrix} \begin{pmatrix} |N(^2P_M)_{\frac{3}{2}^-}\rangle \\ |N(^4P_M)_{\frac{3}{2}^-}\rangle \end{pmatrix}. \quad (7)$$

To show how the coefficients C_{N^*} are related to the mixing angles, we express the amplitudes \mathcal{A}_{N^*} in terms of the product of the meson and photon transition amplitudes:

$$\mathcal{A}_{N^*} \propto \langle N|H_m|N^*\rangle \langle N^*|H_e|N\rangle, \quad (8)$$

where H_m and H_e are the meson and photon transition operators, respectively. Using Eqs. (6) to (8), for the resonance $S_{11}(1535)$ one finds

$$\begin{aligned} \mathcal{A}_{S_{11}(1535)} \propto & \left[\langle N|H_m|N(^2P_M)_{\frac{1}{2}^-}\rangle \cos\theta_S - \langle N|H_m|N(^4P_M)_{\frac{1}{2}^-}\rangle \sin\theta_S \right] \\ & \left[\langle N(^2P_M)_{\frac{1}{2}^-}|H_e|N\rangle \cos\theta_S - \langle N(^4P_M)_{\frac{1}{2}^-}|H_e|N\rangle \sin\theta_S \right] \end{aligned} \quad (9)$$

Due to the Moorhouse selection rule, the amplitude $\langle N(^4P_M)_{\frac{1}{2}^-}|H_e|N\rangle$ vanishes¹⁶ in our model. So, Eq. (9) becomes

$$\begin{aligned} \mathcal{A}_{S_{11}(1535)} \propto & \left[\langle N|H_m|N(^2P_M)_{\frac{1}{2}^-}\rangle \langle N(^2P_M)_{\frac{1}{2}^-}|H_e|N\rangle \right] \\ & \left[\cos^2\theta_S - \sin\theta_S \cos\theta_S \frac{\langle N|H_m|N(^4P_M)_{\frac{1}{2}^-}\rangle}{\langle N|H_m|N(^2P_M)_{\frac{1}{2}^-}\rangle} \right]. \end{aligned} \quad (10)$$

where $\langle N|H_m|N(^2P_M)_{\frac{1}{2}^-}\rangle \langle N(^2P_M)_{\frac{1}{2}^-}|H_e|N\rangle$ determines¹⁶ the CGLN amplitude for the $|N(^2P_M)_{\frac{1}{2}^-}\rangle$ state, and the ratio

$$\mathcal{R} = \frac{\langle N|H_m|N(^4P_M)_{\frac{1}{2}^-}\rangle}{\langle N|H_m|N(^2P_M)_{\frac{1}{2}^-}\rangle}, \quad (11)$$

is a constant determined by the $SU(6) \otimes O(3)$ symmetry. Using the same meson transition operator H_m from the Lagrangian as in deriving the CGLN amplitudes in the quark model, we find $\mathcal{R} = -1$ for the S_{11} resonances and $\sqrt{1/10}$ for the D_{13} resonances. Then, the configuration mixing coefficients can be related to the configuration mixing angles

$$C_{S_{11}(1535)} = \cos\theta_S(\cos\theta_S - \sin\theta_S), \quad (12)$$

$$C_{S_{11}(1650)} = -\sin\theta_S(\cos\theta_S + \sin\theta_S), \quad (13)$$

$$C_{D_{13}(1520)} = \cos\theta_D(\cos\theta_D - \sqrt{1/10}\sin\theta_D), \quad (14)$$

$$C_{D_{13}(1700)} = \sin\theta_D(\sqrt{1/10}\cos\theta_D + \sin\theta_D). \quad (15)$$

3 Results and Discussion

Our effort to investigate the $\gamma p \rightarrow \eta p$ process has gone through three stages.

In our early work¹², we took advantage of the differential cross section data from MAMI⁷ (100 data points for $E_\gamma^{lab} = 0.716$ to 0.790 GeV) and polarization asymmetries measured with polarized target at ELSA⁸ (50 data points for $E_\gamma^{lab} = 0.746$ to 1.1 GeV) and polarized beam at GRAAL⁹ (56 data points for $E_\gamma^{lab} = 0.717$ to 1.1 GeV). Those data allowed us to study the reaction mechanism in the first resonance region and led to the conclusion¹² that the $S_{11}(1535)$ plays by far the major role in this energy range.

Later, differential cross section data were released by the GRAAL collaboration¹⁰ (244 data points for $E_\gamma^{lab} = 0.732$ to 1.1 GeV). Using the four data sets we extended our investigations to the second resonance region and performed a careful treatment of the configuration mixing effects. This work¹³ led us to the conclusion that the inclusion of a new S_{11} resonance was needed to interpret those data.

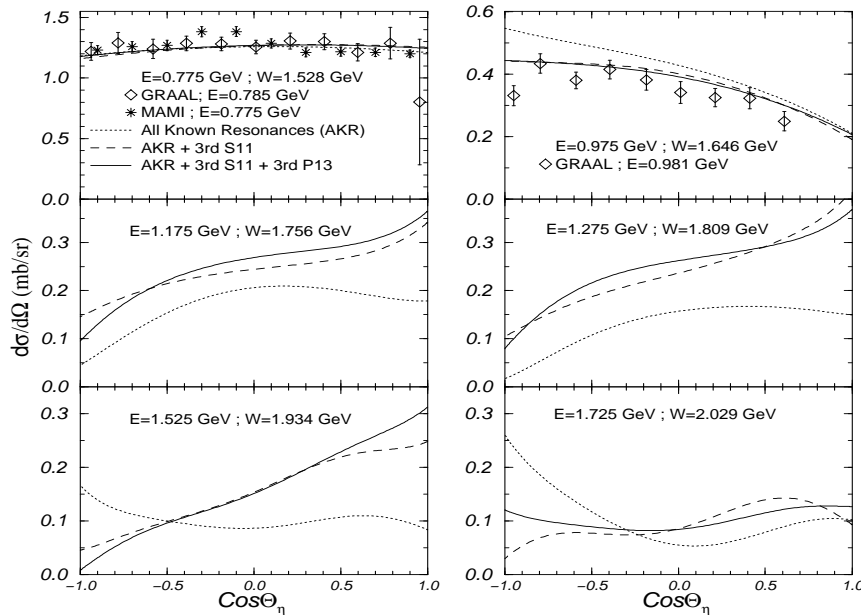
Finally, the third resonance region has just been covered by the CLAS g1a cross section measurements¹¹ (192 data points for $E_\gamma^{lab} = 0.775$ to 1.925 GeV).

Within our approach, we are in the process of interpreting all available experimental results and report here our preliminary findings.

Below, we summarize the main ingredients of the starting point and the used procedure leading to the models \mathcal{M}_1 , \mathcal{M}_2 , and \mathcal{M}_3 (see Table 2 and Figs. 1 to 3):

- **Mixing angles:** Our earlier works^{12,13} have shown the need to go beyond the exact $SU(6) \otimes O(3)$ symmetry. To do so, we used the relations (12) to (15) for the S_{11} and D_{13} resonances and left the mixing angles θ_S and θ_D as free parameters.
- **Model \mathcal{M}_1 :** This model includes explicitly all the eleven known relevant resonances (Table 1) with mass below 2 GeV, while the contributions from the known excited resonances above 2 GeV for a given parity are assumed to be degenerate and hence written in a compact form¹⁵.
- **Model \mathcal{M}_2 :** Because of the poor agreement between the model \mathcal{M}_1 and the data above $E_\gamma^{lab} \approx 1$ GeV, as explained below, and given our previous

Figure 1: Differential cross section for the process $\gamma p \rightarrow \eta p$: angular distribution for $E_\gamma^{\text{lab}} = 0.775$ GeV to 1.725 GeV. The curves come from the models \mathcal{M}_1 (dotted), \mathcal{M}_2 (dashed), and \mathcal{M}_3 (full). Data are from Refs. [7] and [10].



findings¹³, we introduce a third S_{11} resonance with three free parameters (namely the resonance mass, width, and strength).

- **Model \mathcal{M}_3 :** To improve further the agreement between our results and the data, we introduce a third P_{13} missing resonance with three additional adjustable parameters.
- **Fitting procedure:** The free parameters of all the above three models have been extracted using the MINUIT minimization code from the CERN Library. The fitted data base contains roughly 650 values: differential cross-sections from MAMI⁷, GRAAL¹⁰, and JLab¹¹, and the polarization asymmetry data from ELSA⁸ and GRAAL⁹.

In the following, we compare the results of our models with different measured observables^a.

^aThe differential cross sections from JLab¹¹ were kindly provided to us by B. Ritchie and M. Dugger and were included in our fitted data-base. However, given that these data have not yet been published by the CLAS Collaboration, we do not reproduce them here.

Table 2: Results of minimizations for the models as explained in the text.

parameter		\mathcal{M}_1	\mathcal{M}_2	\mathcal{M}_3
Mixing angles:				
	Θ_S	-37°	-34°	-34°
	Θ_D	8°	11°	11°
Third S_{11}	Mass (GeV)		1.795	1.776
	Width (MeV)		350	268
Third P_{13}	Mass (GeV)			1.887
	Width (MeV)			225
$\chi^2_{d.o.f}$		6.5	3.1	2.7

Figure 1 shows our results at six of the CLAS data energies. At the lowest energies we compare our results with data from GRAAL and MAMI. As already mentioned, at the lowest energy the reaction mechanism is dominated by the first S_{11} resonance and the data are equally well reproduced by the three models. At the next shown energy, $E_\gamma^{lab}=0.975$ GeV, we are already in the second resonance region and the model \mathcal{M}_1 overestimates the data, while the models \mathcal{M}_2 and \mathcal{M}_3 improve equally the agreement with the data.

At $E_\gamma^{lab}=1.175$ and 1.275 GeV, the model \mathcal{M}_1 underestimates the unshown JLab data (see footnote a). This is also the case at the two depicted highest energies, except at backward angles, where again the model \mathcal{M}_1 overestimates the JLab data. The reduced χ^2 for this latter model is 6.5, see Table 1.

The most dramatic improvement is obtained by introducing a new S_{11} resonance (Fig. 1, model \mathcal{M}_2), which brings down the reduced χ^2 by more than a factor of 2.

Finally the introduction of a new P_{13} resonance (Fig. 1, model \mathcal{M}_3) gives the best agreement with the data, though it does not play as crucial a role as the third S_{11} resonance.

Predictions of those models for the total cross section, as well as results for the fitted polarizations observables are depicted in Figures 2 and 3, respectively. These theory/data comparisons bolster our conclusions about the new resonances, without providing further selectivity between models \mathcal{M}_2 and \mathcal{M}_3 .

Here, we would like to comment on the values reported in Table 1.

Mixing angles : The extracted values for mixing angles θ_S and θ_D are identical for models \mathcal{M}_2 and \mathcal{M}_3 and differ by 3° from those of the model \mathcal{M}_1 . These values are in agreement with angles determined by Isgur-Karl model⁵

Figure 2: Total cross section as a function of total center-of-mass energy for the process $\gamma p \rightarrow \eta p$; curves and data as in Fig. 1.

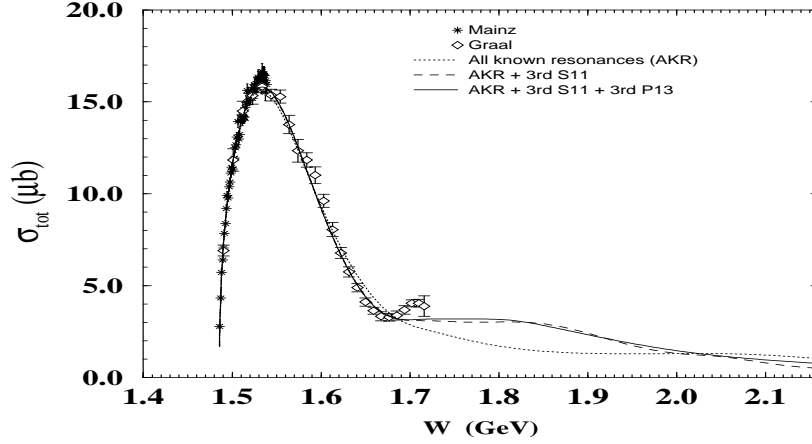
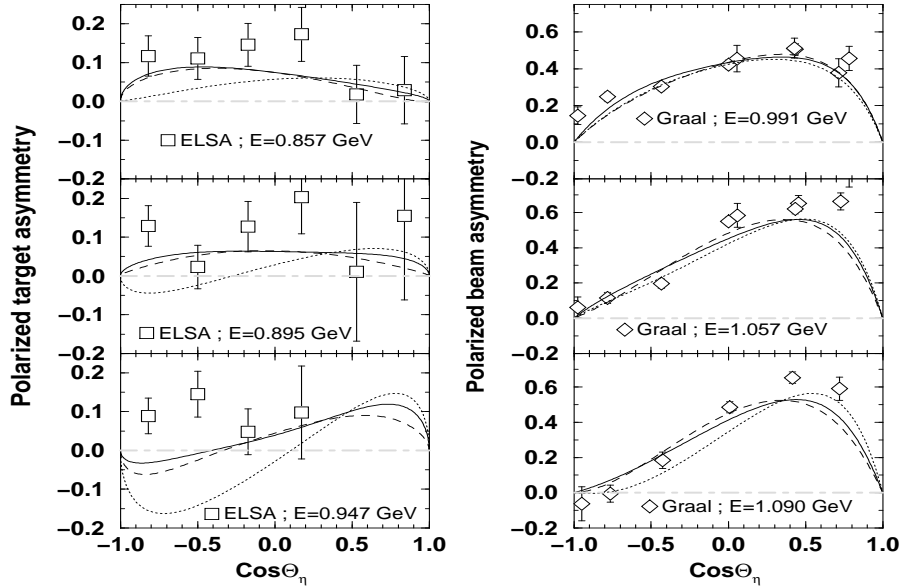


Figure 3: Single polarization asymmetries angular distribution for the process $\gamma p \rightarrow \eta p$; curves as in Fig. 1. Data are from Refs. [8] and [9].



and by large- N_c approaches²⁰.

Third S_{11} resonance: The extracted values for the mass and width of a new S_{11} are close to those predicted by the authors of Ref.¹⁷ ($M=1.712$ GeV and $\Gamma_T=184$ MeV), and our previous findings¹³. Moreover, for the one star $S_{11}(2090)$ resonance¹, the Zagreb group coupled channel analysis¹⁸ produces the following values $M = 1.792 \pm 0.023$ GeV and $\Gamma_T = 360 \pm 49$ MeV. The BES Collaboration reported¹⁹ on the measurements of the $J/\psi \rightarrow p\bar{p}\eta$ decay channel. In the latter work, a partial wave analysis leads to the extraction of the mass and width of the $S_{11}(1535)$ and $S_{11}(1650)$ resonances, and the authors find indications for an extra resonance with $M = 1.800 \pm 0.040$ GeV, and $\Gamma_T = 165^{+165}_{-85}$ MeV. Finally, a recent work⁴ based on the hypercentral constituent quark model predicts a missing S_{11} resonance with $M=1.861$ GeV.

Third P_{13} resonance: The above mentioned hypercentral CQM predicts also three P_{13} resonances with $M=1.816, 1.894,$ and 1.939 GeV. Finally a relativized pair-creation 3P_0 approach³ predicts four missing P_{13} resonances in the relevant energy region with masses between 1.870 and 2.030 GeV.

4 Concluding remarks

We reported here on a study of the process $\gamma p \rightarrow \eta p$ for E_γ^{lab} between threshold and ≈ 2 GeV, using a chiral constituent quark approach.

We show how the symmetry breaking coefficients C_{N^*} are expressed in terms of the configuration mixings in the quark model, thus establish a direct connection between the photoproduction data and the internal quark gluon structure of baryon resonances. The extracted configuration mixing angles for the S and D wave resonances in the second resonance region using a more complete data-base are in good agreement with the Isgur-Karl model⁵ predictions for the configuration mixing angles based on the one gluon exchange, as well as with results coming from the large- N_c effective field theory based approaches²⁰.

However, one of the common features in our investigation of η photoproduction at higher energies is that the existing S-wave resonances can not accommodate the large S-wave component above $E_\gamma^{lab} \approx 1.0$ GeV region. Thus, we introduce a third S-wave resonance in the second resonance region suggested in the literature¹⁷. The introduction of this new resonance, improves significantly the quality of our fit and reproduces very well the cross-section increase in the second resonance region. The quality of our semi-prediction for the total cross-section and our results for the polarized target and beam asymmetries, when compared to the data, gives confidence to the presence of a third S_{11} resonance, for which we extract some static and dynamical properties: $M \approx$

1.776 GeV, $\Gamma_T \approx 268$ MeV. These results are in very good agreement with those in Refs. ^{4,17,19}, and compatible with ones in Ref. ¹⁸. Finally, we find indications for a missing P_{13} resonance^{3,4} with $M \approx 1.887$ GeV, $\Gamma_T \approx 225$ MeV.

Acknowledgments

One of us (BS) wishes to thank the organizers for their kind invitation to this very stimulating symposium. We are indebted to Barry Ritchie and Michael Dugger for having provided us with the CLAS g1a data prior to publication.

References

1. Particle Data Group, *Eur. Phys. J. A* **15**, 1 (2000).
2. S. Capstick, W. Roberts, *Prog. Part. Nucl. Phys.* **45**, 5241 (2000); R. Bijker, F. Iachello, A. Leviatan, *Ann. Phys.* **236**, 69 (1994); *Ann. Phys.* **284**, 89 (2000); L.Ya. Glozman, D.O. Riska, *Phys. Rep.* **268**, 263 (1996); M. Anselmino *et al.*, *Rev. Mod. Phys.* **65**, 1199 (1993).
3. S. Capstick, *Phys. Rev. D* **46**, 2864 (1992); S. Capstick, W. Roberts, *Phys. Rev. D* **49**, 4570 (1994).
4. M.M. Giannini, E. Santopinto, A. Vassalo, nucl-th/0111073.
5. N. Isgur, G. Karl, *Phys. Lett. B* **72**, 109 (1977); N. Isgur, G. Karl, R. Koniuk, *Phys. Rev. Lett.* **41**, 1269 (1978).
6. R. Bijker, F. Iachello, A. Leviatan, *Phys. Rev. C* **54**, 1935 (1996).
7. B. Krusche *et al.*, *Phys. Rev. Lett.* **74**, 3736 (1995).
8. A. Bock *et al.*, *Phys. Rev. Lett.* **81**, 534 (1998).
9. J. Ajaka *et al.*, *Phys. Rev. Lett.* **81**, 1797 (1998).
10. F. Renard *et al.*, submitted to *Phys. Lett. B*, hep-ex/0011098.
11. M. Dugger, B. Ritchie *et al.* (CLAS Collaboration), to be submitted to *Phys. Rev. Lett.*; B. Ritchie, private communication (Oct. 01).
12. Z. Li, B. Saghai, *Nucl. Phys. A* **644**, 345 (1998).
13. B. Saghai, Z. Li, *Eur. Phys. J. A* **11**, 217 (2001).
14. A. Manohar, H. Georgi, *Nucl. Phys. B* **234**, 189 (1984).
15. Z. Li, *Phys. Rev. D* **48**, 3070 (1993); *Phys. Rev. D* **50**, 5639 (1994); *Phys. Rev. C* **52**, 1648 (1995).
16. Z. Li, H. Ye, M. Lu, *Phys. Rev. C* **56**, 1099 (1997).
17. Z. Li, R. Workman, *Phys. Rev. C* **53**, R549 (1996).
18. M. Batinić *et al.*, *Phys. Scripta* **58**, 15 (1998); A. Švarc, S. Ceci, nucl-th/0009024.
19. J.Z. Bai *et al.* (BES Collaboration), *Phys. Lett. B* **510**, 75 (2001).
20. D. Pirjol, T.-M. Yan, *Phys. Rev. D* **57**, 5434 (1998); C.E. Carlson *et al.*, *Phys. Rev. D* **59**, 114008 (1999).